Published in final edited form as:

Stroke. 2019 October ; 50(10): 2761–2767. doi:10.1161/STROKEAHA.119.025738.

Brain connectivity measures improve modeling of functional outcome after acute ischemic stroke

Sofia Ira Ktena, PhD[1,2,*], **Markus D. Schirmer, PhD**[1,3,4,*], **Mark R. Etherton, MD, PhD**[1], **Anne-Katrin Giese, MD**[1], **Carissa Tuozzo, BA**[1], **Brittany B Mills, BSc**[1], **Daniel Rueckert, PhD**[2], **Ona Wu, PhD**[5], **Natalia S. Rost, MD, MPH, FAAN**[1]

[1]Stroke Division & Massachusetts General Hospital, J. Philip Kistler Stroke Research Center, Harvard Medical School, Boston, USA

[2]Biomedical Image Analysis Group, Imperial College London, London, UK

[3]Computer Science and Artificial Intelligence Lab, Massachusetts Institute of Technology, Boston, USA

[4]Department of Population Health Sciences, German Centre for Neurodegenerative Diseases (DZNE), Germany

[5]Athinoula A. Martinos Center for Biomedical Imaging, Department of Radiology, Massachusetts General Hospital, Charlestown, MA, USA

Abstract

Background and Purpose: The ability to model long-term functional outcomes after acute ischemic stroke (AIS) represents a major clinical challenge. One approach to potentially improve prediction modeling involves the analysis of connectomics. The field of connectomics represents the brain's connectivity as a graph, whose topological properties have helped uncover underlying mechanisms of brain function in health and disease. Specifically, we assessed the impact of stroke lesions on rich club (RC) organization, a high capacity backbone system of brain function.

Methods: In a hospital-based cohort of 41 AIS patients, we investigated the effect of acute infarcts on the brain's pre-stroke RC backbone and post-stroke functional connectomes with respect to post-stroke outcome. Functional connectomes were created utilizing three anatomical atlases and characteristic path-length (L) was calculated for each connectome. The number of RC regions (N_{RC}) affected were manually determined using each patient's diffusion weighted image (DWI). We investigated differences in L with respect to outcome (modified Rankin Scale score (mRS); 90-days) and the National Institutes of Health Stroke Scale (NIHSS; early: 2–5 days; late: 90-day follow-up). Furthermore, we assessed the effect of including N_{RC} and L in 'outcome' models, using linear regression and assessing the explained variance (R^2).

Results: Of 41 patients (mean age (range): 70 (45–89) years), 61% were male. Lower L was generally associated with better outcome. Including N_{RC} in the backward selection models of

Corresponding author: M.D. Schirmer, JPK Stroke Research Center, MGH, 175 Cambridge Street, Suite 300, Boston, MA-02114, USA, Tel:6176437597;Fax:6176433939, mschirmer1@mgh.harvard.edu, Twitter:@schirmermd;@nsanar.
*Authors contributed equally.

outcome, R^2 increased between 1.3- and 2.6-fold beyond that of traditional markers (age and acute lesion volume) for NIHSS and mRS.

Conclusions: In this proof-of-concept study, we showed that information on network topology can be leveraged to improve modeling of post-stroke functional outcome. Future studies are warranted to validate this approach in larger prospective studies of outcome prediction in stroke.

Keywords

brain connectivity; ischemic stroke; functional outcome; clinical outcome; network topology; Ischemic Stroke; Functional Magnetic Resonance Imaging (fMRI); Biomarkers

Introduction

Stroke is a leading cause of long-term adult disability[1] with significant public health burden[2]. Importantly, the ability to individually prognosticate stroke outcomes in the acute setting remains challenging[3], due to the complex mechanisms of post-stroke recovery[4].

Magnetic resonance imaging (MRI) allows the mapping of anatomical regions and their interconnection through diffusion weighted imaging (DWI) or functional co-activation (e.g. resting state functional MRI (rsfMRI)). Connectomics describes the brain as a graph and allows the exploration of brain connectivity with network theoretical measures[5]. This has led to fundamental insights into the brain's organization[6–8], resilience to injury[9], and alterations due to disease[10]. Associations between structural features and functional post-stroke outcome have recently been established[11]. However, the effect of premorbid structural and/or functional brain connectivity organization on recovery after stroke and its role in resilience to damage is yet to be fully elucidated.

A so-called rich club (RC) organization has been described in the human connectome[6,8], comprising a set of regions which are thought to form an information backbone, crucial for brain function, and susceptible to disease[12]. Van den Heuvel and Sporns[6] identified six bilateral regions belonging to the RC, mediating long-distance connections between brain modules[13], and demonstrating their critical role for cognition[14] and behavior[15]. Localized damage to their connections significantly impacts global network efficiency[6] and have been shown to lead to functional deficits in disorders like Alzheimer's disease[16]. Stroke location has also been identified as an independent determinant of outcome[17], in addition to clinical factors, such as age[18] and lesion size[19]. Furthermore, a strong coupling between brain hubs and regional blood flow has been unveiled during rest and in response to task demands[20]. The effect of focal injury on brain networks has been recently explored[21], however, without a clear mapping between lesion location and its topological network characteristics. Functional connectivity has been investigated in longitudinal studies of motor recovery after stroke[22] and significant correlations between interhemispheric resting-state connections and functional performance have been identified[23,24]. Nevertheless, the effect of focal ischemic stroke lesions on whole-brain functional organization estimated before and after stroke have not been investigated.

In this study, we examine the functional network organization in AIS patients and the lesion location in relation to network topology with respect to functional outcome. Here, we assessed the impact of ischemic insults on brain regions that constitute the RC backbone, as well as functional network topology at a global level, in a prospective, hospital-based cohort. We hypothesize that models incorporating connectivity information, specifically characteristic path length in the acute phase and the number of RC regions affected by the stroke lesion, will improve AIS outcome models. Using multivariate linear regression, we investigated, if connectivity metrics obtained early in the course of AIS, and with the potential to be acquired at time of admission, can improve understanding of the mechanisms underlying variability in post-stroke functional outcomes.

Materials and Methods

The authors agree to make available to any researcher the data, methods used in the analysis, and materials used to conduct the research for the express purposes of reproducing the results and with the explicit permission for data sharing by the local institutional review board.

Patient population

AIS patients were enrolled in the SALVO (Statins augment small vessel function and improve stroke outcomes) study after admission to the Emergency Department at Massachusetts General Hospital. The study was approved by the Institutional Review Board and all participants, or their surrogates, gave written informed consent at the time of enrolment. AIS was defined as: (a) acute onset of focal neurological symptoms consistent with cerebrovascular syndrome, (b) MRI findings consistent with acute cerebral ischemia, and (c) no evidence of other neurological disorders to explain the symptoms. Subjects with moderate to severe white matter hyperintensity (WMH) burden (Fazekas grade ≥2) were eligible for enrolment and participants with medical contraindications to gadolinium-based contrast agents were excluded from this study.

Clinical assessment

Upon admission to the hospital, the National Institutes of Health Stroke Scale score (NIHSS; 0 (no symptoms) - 42) was recorded for each patient by a trained neurologist. Utilizing NIHSS as a pseudo outcome score, post-stroke functional outcome was assessed during two follow-up assessments: (1) within 2–5 days after admission (average 2.6 days, “early” in-hospital follow-up) and (2) at 90 days (“late” follow-up). Additionally, the modified Rankin Scale score (mRS; 0 (no symptoms) - 6 (death)) was recorded at late follow-up. For each patient, mRS was determined in an interview with the patient or health care proxy, including pre-stroke mRS.

Data acquisition

Patients enrolled in the SALVO study underwent a research protocol MRI, including structural, diffusion and functional imaging, in the hospital at 2–5 days after admission. A T1-weighted image (in-plane resolution, 0.430 mm; slice thickness, 6mm; matrix size, 480×512; number of slices, 28), and gradient-echo echoplanar imaging (EPI) data depicting

blood oxygen level-dependent contrast at rest were acquired at 3.0T in Massachusetts General Hospital (Boston, USA). The rsfMRI data (N=33) consisted of 150 volumes (number of slices, 42 (interleaved); slice thickness, 3.51 mm; matrix size, 64×64; flip angle, 90°; repetition time (TR), 2400 ms; in-plane resolution, 3.437 mm). In the majority of subjects, DWI was performed using a 3T (Siemens Skyra; numbers of slices, 28; slice thickness, 5mm; TR, 5500 ms; TE, 99ms; in-plane resolution, 1.375mm). For five of the patients in this cohort 1.5T MRI was used due to medical contraindications for 3T, such as the presence of a pacemaker.

Image processing

Structural and functional images were preprocessed using the Configurable Pipeline for the Analysis of Connectomes[25], including bias field correction[26], brain extraction[27], non-linear registration[28] to the MNI (Montreal Neurological Institute) anatomical template. Cerebrospinal fluid (CSF), grey and white matter masks were generated using FSL FAST[29].

Functional data underwent slice timing correction and geometrical displacements due to head movement were corrected (rigid registration; AFNI software (https://afni.nimh.nih.gov/)). Brain extraction was performed using FSL BET[30]. Each patient's 150 functional images were affinely registered to the T1 image in MNI space, and underwent mean intensity normalization. Finally, nuisance signal regression was performed for white matter, CSF and global mean, and the functional time series were band-pass filtered (0.01–0.1Hz) and scrubbed for extreme frame displacement (>3mm). Preprocessing steps are summarized in Figure 1.

Rich club region characterization

Rich-club regions can either be determined by directly calculating it from connectivity matrices (see Appendix AI), or by utilizing prior regions. Van den Heuvel and Sporns[6] identified a set of RC regions, characterized by high connection strength, high centrality and efficient information transmission. This set comprises 6 bilateral regions, including the *precuneus*, *superior frontal* and *parietal cortex*, *putamen*, *hippocampus* and *thalamus* (see Figure 2A). In our study, an expert neurologist (M.R.E.), blinded to outcomes, manually identified the number of RC regions affected by the lesion (N_{RC}) and outlined the acute infarct lesions on the DWI image.

Network analysis of functional connectivity

Three anatomical atlases (Destrieux[31] (Des), Harvard-Oxford[32] (HO), and AAL atlas[33]) were used to define brain regions, allowing us to explore reproducibility of the findings across different brain parcellations. For each set of regions, mean time series were calculated and strengths of the connections were estimated using partial correlations[34]. Global network efficiency was estimated via characteristic path length[5], L_{atlas}^{weight}, for each atlas and connectivity weight. L describes the average 'distance' between regions and is inversely related to the observed functional correlations in the data. In this study, we retain positive, negative and absolute weights of the estimated networks, as there is no consensus on which of these is most discriminative.

Functional topology and outcome models

We investigated associations between N_{RC} and outcome using the Spearman's correlation coefficient (ρ), as well as differences in *L* with respect to NIHSS using Pearson's correlation coefficient (r).

Subsequently, we modeled outcome using linear regressions based on age, lesion volume (DWIv), NIHSS at admission ($NIHSS_{adm}$), pre-stroke mRS (mRS_{pre}), *L* and N_{RC}. First, we performed a univariate analysis. For multivariate analysis, we defined the *baseline model* based on age, DWIv, and *early outcome measures* ($NIHSS_{adm}$ or mRS_{pre}, for outcome models based on NIHSS and mRS, respectively). In the *initial model*, we further included N_{RC} and *L*, with interactions between N_{RC} and DWIv (larger lesions are likely to affect more RC regions), as well as N_{RC} and *L* (damage to RC regions leads to larger disturbance in network efficiency, and therefore *L*). To reduce the statistical burden of the model, we performed backward elimination, iteratively removing variables with the highest p-value above 0.05. This reduced model is referred to as outcome model. Models incorporate information related to both structural and functional connectivity, however, as *L* is only available for patients with available fMRI data, we remove it after backward elimination to test the model in the larger cohort. The baseline and initial models are given as

$$\text{Outcome} \sim \text{Age} + \text{DWIv} + \text{early outcome measure}$$

and

$$\text{Outcome} \sim \text{Age} + \text{DWIv} + N_{RC} + L + \text{DWIv}:N_{RC} + N_{RC}:L + \text{early outcome measure},$$

respectively, where interaction terms are indicated by ':'.

Models are evaluated using explained variance (with (R^2_{adj}) and without (R^2) adjustment for the number of independent variables), as well as the Akaike (AIC) and Bayes information criterion (BIC), where smaller values correspond to better model fit. Differences in the information criterion greater than 10 furthermore suggest strong support of the model with the lower value over the model with the higher value[35,36]. All analyses were performed using the computing environment R[37].

Results

Forty-four AIS patients were enrolled in this study. Three patients were subsequently excluded because the MRI was not obtained. Of the remaining 41 patients (summarized in Table 1), all had $NIHSS_{adm}$, $NIHSS_{early}$, and mRS recorded. For 28 patients 90-day NIHSS score was also obtained and fMRI data was collected for 33 patients.

Associations between functional outcome and network topology

Figure 2B characterizes outcomes in our cohort. We observed a positive correlation between all outcome measures and N_{RC} (ρ=0.54, 0.58, and 0.58 for $NIHSS_{early}$, $NIHSS_{late}$, and mRS, respectively (all $p<0.001$); see Figure 2B/C).

We explored *L* for positive weights (see Table 1 and Table I). Additionally, we found a positive correlation between $NIHSS_{early}$ and *L*, as well as mRS and L, for all atlases ($NIHSS_{early}$: r_{HO}=0.42 (p=0.01), r_{AAL}=0.38 (p=0.03), and r_{Des}=0.41 (p=0.02); mRS: r_{HO}=0.49 (p<0.01), r_{AAL}=0.44 (p=0.01), and r_{Des}=0.47 (p<0.01); see Figure I).

Outcome model based on connectivity measures

Univariate analysis showed that all factors were significant for all outcome measures, except for mRS_{pre} in case of the 90-day NIHSS score (see Table II). Utilizing the initial model in the multivariate analysis, we compared each outcome to its corresponding baseline model (Table 2) after backward elimination (Table III).

Models including connectivity information showed the highest R^2 (both unadjusted and adjusted) and lowest AIC and BIC with differences greater than 10, compared to the baseline models. Specifically, including both N_{RC} and *L* resulted in a 1.3-, 2.6-, and 1.3-fold increase in explained variance over the baseline model for $NIHSS_{early}$, $NIHSS_{late}$, and mRS, respectively. Importantly, models after removing *L*, and thereby extending it to the bigger cohort where no fMRI data was available, perform similarly or outperform their corresponding baseline models. Including treatment as a 'nuisance' variable in the models did not change model performance (p>0.2).

Discussion

Functional outcomes vary significantly in the early and late phases of stroke recovery and are difficult to model at AIS onset. Using the acute stroke lesions visible on the admission DWI, we demonstrated the importance of the integrity of the RC backbone on functional outcomes after AIS, by means of N_{RC}, and its association with early and late functional outcome. Additionally, we showed that the topology of functional networks significantly augments outcome models.

Our results align with findings in the literature. Munsch et al.[38] identified stroke location as an independent determinant of cognitive outcome measured at 3 months post-stroke. Similar results were demonstrated by Wu et al.[17], highlighting the importance of joint modelling of DWI volume and topography for stroke outcomes, while our approach also takes network topology into account. Other studies have indicated correlations between network topology and stroke recovery. Wang et al.[39] showed that stroke patients exhibit higher network segregation compared to healthy controls and demonstrated an association with restoration of function. Cheng et al.[40] investigated whole-brain functional network organization in a cohort of 12 stroke patients with motor deficits from 10 days to 3 months post-stroke and showed decreased network integration (higher *L*) for patients with right-hemispheric stroke during an ipsilateral finger tapping task. This further agrees with our results, where patients with worse outcome showed higher values of *L*.

Rich club regions comprise brain areas responsible for distributing a large fraction of the brain's neural communications, underpinning their importance for recovery. The underlying physiological causes of this phenomenon can be explained by (1) the disproportionate impact of pathological attacks on brain hubs on the global efficiency of information

processing[41], (2) the increased vulnerability of these regions to pathogenic factors, due to their topological centrality and high biological cost manifested by their long-distance neuronal connections, and/or (3) the brain's inability to compensate for damage or loss of these regions. The outcome model was further improved after introducing a measure of functional network efficiency (L), which directly describes how focal lesions affect the brain network at a global level. After backward elimination in two of the three models only the interaction term between L and N_{RC} remained. This suggests that the importance of these regions for functional outcome increases, as efficiency of the brain network decreases (larger L). In this case, L after stroke might serve as a surrogate measure of L before the stroke and future studies are required to disentangle a causal relationship. However, information on L before stroke are difficult to obtain. Regardless, comparing the associations between L and outcome highlights that a more intact and/or efficient network communication in the acute phase of stroke is associated with better outcome. While the mechanisms through which the brain's functional reorganization facilitates recovery after stroke and the causal relationship between the two variables are yet to be explored, our findings indicate that L, estimated from rsfMRI in the acute stroke phase, may be utilized as a determinant of functional recovery.

These results underscore the importance of efficient brain connectivity in functional recovery and resilience to brain damage after ischemic stroke. Our model accounts for some of the most commonly reported confounding factors that are available in the acute setting, i.e. age and lesion volume. We found that, although N_{RC} is correlated with DWIv, the volume alone is not enough to explain the early and late outcomes as measured by the NIHSS score. Despite the positive correlation between these two measures (ρ=0.46), there are both large infarcts that do not affect any RC regions and small infarcts that involve one or two RC regions, demonstrating that a larger DWIv does not equal greater N_{RC}. In future work, we aim to investigate whether the incorporation of structural connectivity measures could further improve modeling of long-term functional outcome. As suggested by Carter et al.[23], each behavioral deficit and its variability across stroke patients will likely be explained by a combination of structural variables (e.g. DWIv) and their interaction with measures of structural (e.g. integrity of white matter pathways), and functional connectivity. This is supported by our resulting models after backward elimination, where the models of NIHSS incorporate age or DWIv, as well as measures of structural (N_{RC}) and functional (L) connectivity.

Here, we observed an increase in R^2 in the outcome model of early NIHSS, where the model using age and connectome information outperform a model using the same measure obtained 2–5 days earlier. While the connectome information remain in the model, age loses its significance and DWIv becomes more important in the late NIHSS assessment. This suggests that age plays an important role in compensating acute effects of stroke, whereas effects of structural damage (DWIv) become more important for long-term outcome and recovery. While rsfMRI data is often not available in the hyper-acute stage of stroke, we removed L from our models, demonstrating a clinically relevant and easy to assess model. Even without L, the presented models demonstrated an increase in R^2 over their corresponding baseline models, except for mRS. However, mRS is the only model not containing either age or DWIv. Re-introducing age into the model, as it was the last parameter removed during backward elimination, results in both age and N_{RC} being

significant with explained variance of R^2=0.66, showing similar improvement to NIHSS models.

There are limitations that need to be taken into consideration when interpreting these results. First, regional delays have been identified in rsfMRI fluctuations in stroke patients (hemodynamic lag) due to vascular occlusion[42]. Approaches have been proposed to correct for such lags[43], however, there is no consensus on how to address this challenge. Importantly, this effect may be an integral part of the observed differences between outcomes. Another limitation results from potential registration errors, due to relatively low through-plane resolution of and pathology within the anatomical scans. While registration errors increase noise in the analysis, it is unlikely that this will cause a systematic error in our cohort of patients with right- (N=22) and left-hemispheric (N=11) strokes. Moreover, by using three atlases to investigate functional network topology and demonstrating consistent trends, our results are less prone to systematic errors due to misalignment of boundaries between regions. In this study, a subset of patients (N=5) had contraindication for 3T MRI acquisition and subsequently underwent 1.5T imaging. However, studies suggest that there are no significant differences in the assessment of lesion volume between 1.5T and 3T systems in the hyperacute stage[44]. Generally, this study presents a proof-of-concept, due to the relatively small sample size. Specifically, only few subjects showed poor outcome, which can affect model fit, as these might be considered ‘outliers’. While the assumptions of the linear models were fulfilled, we observed a quantile-quantile plot corresponding to a heavy-tailed distribution of the standardized residuals. However, after excluding subjects with ‘extreme’ outcomes ($NIHSS_{early}$>15, $NIHSS_{late}$>9, and mRS of 5), thereby improving model fit, results remained consistent and demonstrated an increase in explained variance. Moreover, mRS is usually modeled using ordinal regressions, requiring larger datasets than was available in this study. Considering the agreement with outcome models using NIHSS in terms of retained factors, however, we do not expect a significant change in retained factors, as using linear regression is more likely to introduce more noise in the data. Future studies with larger cohorts, may explore more complex models, utilizing additional phenotypic information, and investigate the potential for creating appropriate prediction models.

Among the strengths of this study was the thoroughly ascertained and well-characterized hospital-based dataset of patients with AIS and consecutive assessments of functional post-stroke outcomes. These included consecutive outcome measurements of NIHSS, which is a fine-grained measure of impairment after stroke. Importantly, in combining N_{RC} and topological information from functional connectivity, we were able to interrogate effects on both the structural (N_{RC}) and functional (L) brain networks, combining them into a single, intuitive outcome model.

Summary

In conclusion, this is the first study exploring functional network and RC topology of brain connectivity in AIS patients, as well as their association with early and late post-stroke outcomes. Our findings highlight the impact of stroke location on functional recovery, as well as the importance of structural connectivity hubs and functional integration for efficient information transmission. The proposed model yields a 1.3–2.6-fold improvement in

explained variance over the baseline model, improving our understanding of how stroke affects functional brain organization in the acute setting.

Supplementary Material

Refer to Web version on PubMed Central for supplementary material.

Acknowledgments

Source of Funding

This work was funded by NIH Grant 5R01NS082285 (SALVO study, Rost PI). Sofia Ira Ktena was supported by the Engineering and Physical Sciences Research Council Centre for Doctoral Training in High Performance Embedded and Distributed Systems (High Performance Embedded and Distributed Systems, Grant EP/L016796/1; Rueckert PI) and an European Molecular Biology Organization short-term fellowship (7284). Markus D. Schirmer was supported by the European Union's Horizon 2020 research and innovation programme under the Marie Sklodowska-Curie grant agreement No 753896. Mark R. Etherton was supported by American Heart Association Grant 17CPOST33680102.

Disclosures:

Dr Ktena has nothing to disclose.

Dr Schirmer reports grants from the European Union's Horizon2020 framework during the conduct of the study.

Dr Etherton reports grants from American Heart Association during the conduct of the study.

Dr Giese has nothing to disclose.

Dr Tuozzo has nothing to disclose.

Ms. Mills reports grants from NIH/National Institute of Neurological Disorders and Stroke during the conduct of the study.

Dr Rueckert report s grant s and personal fees from Heart flow, personal fees from Circle Cardiovascular Imaging, and personal fees from IXICO outside the submitted work.

Dr Wu reports grants from NIH/National Institute of Neurological Disorders and Stroke during the conduct of the study; grants from American Heart Association, personal fees from Penumbra, and personal fees from Genentech outside the submitted work.

Dr Rost reports grants from NIH/National Institute of Neurological Disorders and Stroke during the conduct of the study; personal fees from Broadview Ventures, personal fees from Genzyme Sanofi, personal fees from Abbvie, personal fees from Omniox, and personal fees from Covance outside the submitted work.

References

1. Feigin VL, Forouzanfar MH, Krishnamurthi R, Mensah GA, Connor M, Bennett DA, et al. Global and regional burden of stroke during 1990–2010: findings from the Global Burden of Disease Study 2010. The Lancet 2014;383:245–255.
2. Di Carlo A. Human and economic burden of stroke Oxford University Press; 2009.
3. Counsell C, Dennis M. Systematic review of prognostic models in patients with acute stroke. Cerebrovasc. Dis 2001;12:159–170. [PubMed: 11641579]
4. Meschia JF. Addressing the heterogeneity of the ischemic stroke phenotype in human genetics research. Stroke 2002;33:2770–2774. [PubMed: 12468768]
5. Rubinov M, Sporns O. Complex network measures of brain connectivity: uses and interpretations. Neuroimage 2010;52:1059–1069. [PubMed: 19819337]
6. Van Den Heuvel MP, Sporns O. Rich-club organization of the human connectome. J. Neurosci 2011;31:15775–15786. [PubMed: 22049421]

7. Ktena SI, Arslan S, Parisot S, Rueckert D. Exploring heritability of functional brain networks with inexact graph matching. In: Biomedical Imaging (ISBI 2017), 2017 IEEE 14th International Symposium on. IEEE; 2017 p. 354–357.
8. Schirmer MD, Chung AW, Grant PE, Rost NS. Network structural dependency in the human connectome across the life span. Network Neuroscience 2018;1–15
9. Achard S, Salvador R, Whitcher B, Suckling J, Bullmore ED. A resilient, low-frequency, small-world human brain functional network with highly connected association cortical hubs. J. Neurosci 2006;26:63–72. [PubMed: 16399673]
10. Fornito A, Zalesky A, Breakspear M. The connectomics of brain disorders. Nat. Rev. Neurosci 2015;16:159. [PubMed: 25697159]
11. Etherton MR, Wu O, Cougo P, Giese A-K, Cloonan L, Fitzpatrick KM, et al. Integrity of normal-appearing white matter and functional outcomes after acute ischemic stroke. Neurology 2017;10–1212.
12. van den Heuvel MP, Sporns O, Collin G, Scheewe T, Mandl RC, Cahn W, et al. Abnormal rich club organization and functional brain dynamics in schizophrenia. JAMA Psychiatry 2013;70:783–792. [PubMed: 23739835]
13. Zamora-López G, Zhou C, Kurths J. Cortical hubs form a module for multisensory integration on top of the hierarchy of cortical networks. Front. Neuroinformatics 2010;4:1.
14. Crossley NA, Mechelli A, Vértes PE, Winton-Brown TT, Patel AX, Ginestet CE, et al. Cognitive relevance of the community structure of the human brain functional coactivation network. Proc. Natl. Acad. Sci 2013;110:11583–11588. [PubMed: 23798414]
15. van den Heuvel MP, Kahn RS, Goñi J, Sporns O. High-cost, high-capacity backbone for global brain communication. Proc. Natl. Acad. Sci 2012;109:11372–11377. [PubMed: 22711833]
16. Crossley NA, Mechelli A, Scott J, Carletti F, Fox PT, McGuire P, et al. The hubs of the human connectome are generally implicated in the anatomy of brain disorders. Brain 2014;137:2382–2395. [PubMed: 25057133]
17. Wu O, Cloonan L, Mocking SJ, Bouts MJ, Copen WA, Cougo-Pinto PT, et al. Role of acute lesion topography in initial ischemic stroke severity and long-term functional outcomes. Stroke 2015;46:2438–2444. [PubMed: 26199314]
18. Jokinen H, Melkas S, Ylikoski R, Pohjasvaara T, Kaste M, Erkinjuntti T, et al. Post-stroke cognitive impairment is common even after successful clinical recovery. Eur. J. Neurol 2015;22:1288–1294. [PubMed: 26040251]
19. Vogt G, Laage R, Shuaib A, Schneider A. Initial lesion volume is an independent predictor of clinical stroke outcome at day 90: an analysis of the Virtual International Stroke Trials Archive (VISTA) database. Stroke 2012;43:1266–1272. [PubMed: 22403046]
20. Liang X, Zou Q, He Y, Yang Y. Coupling of functional connectivity and regional cerebral blood flow reveals a physiological basis for network hubs of the human brain. Proc. Natl. Acad. Sci 2013;110:1929–1934. [PubMed: 23319644]
21. Aerts H, Fias W, Caeyenberghs K, Marinazzo D. Brain networks under attack: robustness properties and the impact of lesions. Brain 2016;139:3063–3083. [PubMed: 27497487]
22. Park C, Chang WH, Ohn SH, Kim ST, Bang OY, Pascual-Leone A, et al. Longitudinal changes of resting-state functional connectivity during motor recovery after stroke. Stroke 2011;STROKEAHA–110.
23. Carter AR, Astafiev SV, Lang CE, Connor LT, Rengachary J, Strube MJ, et al. Resting interhemispheric functional magnetic resonance imaging connectivity predicts performance after stroke. Ann. Neurol 2010;67:365–375. [PubMed: 20373348]
24. Rehme AK, Grefkes C. Cerebral network disorders after stroke: evidence from imaging-based connectivity analyses of active and resting brain states in humans. J. Physiol 2013;591:17–31. [PubMed: 23090951]
25. Sikka S, Cheung B, Khanuja R, Ghosh S, Yan C, Li Q, et al. Towards automated analysis of connectomes: The configurable pipeline for the analysis of connectomes (c-pac). In: 5th INCF Congress of Neuroinformatics, Munich, Germany 2014.
26. Tustison NJ, Avants BB, Cook PA, Zheng Y, Egan A, Yushkevich PA, et al. N4ITK: improved N3 bias correction. IEEE Trans. Med. Imaging 2010;29:1310–1320. [PubMed: 20378467]

27. Schirmer MD, Dalca AV, Sridharan R, Giese A-K, Donahue KL, Nardin MJ, et al. White matter hyperintensity quantification in large-scale clinical acute ischemic stroke cohorts–The MRI-GENIE study. NeuroImage: Clinical 2019;101884. [PubMed: 31200151]
28. Avants BB, Tustison NJ, Song G, Cook PA, Klein A, Gee JC. A reproducible evaluation of ANTs similarity metric performance in brain image registration. Neuroimage 2011;54:2033–2044. [PubMed: 20851191]
29. Woolrich MW, Jbabdi S, Patenaude B, Chappell M, Makni S, Behrens T, et al. Bayesian analysis of neuroimaging data in FSL. Neuroimage 2009;45:S173–S186. [PubMed: 19059349]
30. Smith SM. Fast robust automated brain extraction. Hum. Brain Mapp 2002;17:143–155. [PubMed: 12391568]
31. Fischl B, Van Der Kouwe A, Destrieux C, Halgren E, Ségonne F, Salat DH, et al. Automatically parcellating the human cerebral cortex. Cereb. Cortex 2004;14:11–22. [PubMed: 14654453]
32. Desikan RS, Ségonne F, Fischl B, Quinn BT, Dickerson BC, Blacker D, et al. An automated labeling system for subdividing the human cerebral cortex on MRI scans into gyral based regions of interest. Neuroimage 2006;31:968–980. [PubMed: 16530430]
33. Tzourio-Mazoyer N, Landeau B, Papathanassiou D, Crivello F, Etard O, Delcroix N, et al. Automated anatomical labeling of activations in SPM using a macroscopic anatomical parcellation of the MNI MRI single-subject brain. Neuroimage 2002;15:273–289. [PubMed: 11771995]
34. Richiardi J, Achard S, Bunke H, Van De Ville D. Machine learning with brain graphs: predictive modeling approaches for functional imaging in systems neuroscience. IEEE Signal Process. Mag 2013;30:58–70.
35. Burnham KP, Anderson DR. Multimodel inference: understanding AIC and BIC in model selection. Sociological Methods & Research 2004;33:261–304.
36. Kass RE, Raftery AE. Bayes factors. Journal of the American Statistical Association 1995;90:773–795.
37. R Core Team. R: A language and environment for statistical computing Vienna, Austria: 2018.
38. Munsch F, Sagnier S, Asselineau J, Bigourdan A, Guttmann CR, Debruxelles S, et al. Stroke location is an independent predictor of cognitive outcome. Stroke 2016;47:66–73. [PubMed: 26585396]
39. Wang L, Yu C, Chen H, Qin W, He Y, Fan F, et al. Dynamic functional reorganization of the motor execution network after stroke. Brain 2010;133:1224–1238. [PubMed: 20354002]
40. Cheng L, Wu Z, Fu Y, Miao F, Sun J, Tong S. Reorganization of functional brain networks during the recovery of stroke: a functional MRI study. In: 2012 Annual International Conference of the IEEE Engineering in Medicine and Biology Society. IEEE; 2012 p. 4132–4135.
41. Albert R, Jeong H, Barabási A-L. Error and attack tolerance of complex networks. nature 2000;406:378. [PubMed: 10935628]
42. Siegel JS, Shulman GL, Corbetta M. Measuring functional connectivity in stroke: approaches and considerations. Journal of Cerebral Blood Flow & Metabolism 2017;37:2665–2678. [PubMed: 28541130]
43. Siegel JS, Snyder AZ, Ramsey L, Shulman GL, Corbetta M. The effects of hemodynamic lag on functional connectivity and behavior after stroke. Journal of Cerebral Blood Flow & Metabolism 2016;36:2162–2176. [PubMed: 26661223]
44. Kosior RK, Wright CJ, Kosior JC, Kenney C, Scott JN, Frayne R, et al. 3-Tesla versus 1.5-Tesla magnetic resonance diffusion and perfusion imaging in hyperacute ischemic stroke. Cerebrovascular Diseases 2007;24:361–368. [PubMed: 17690549]

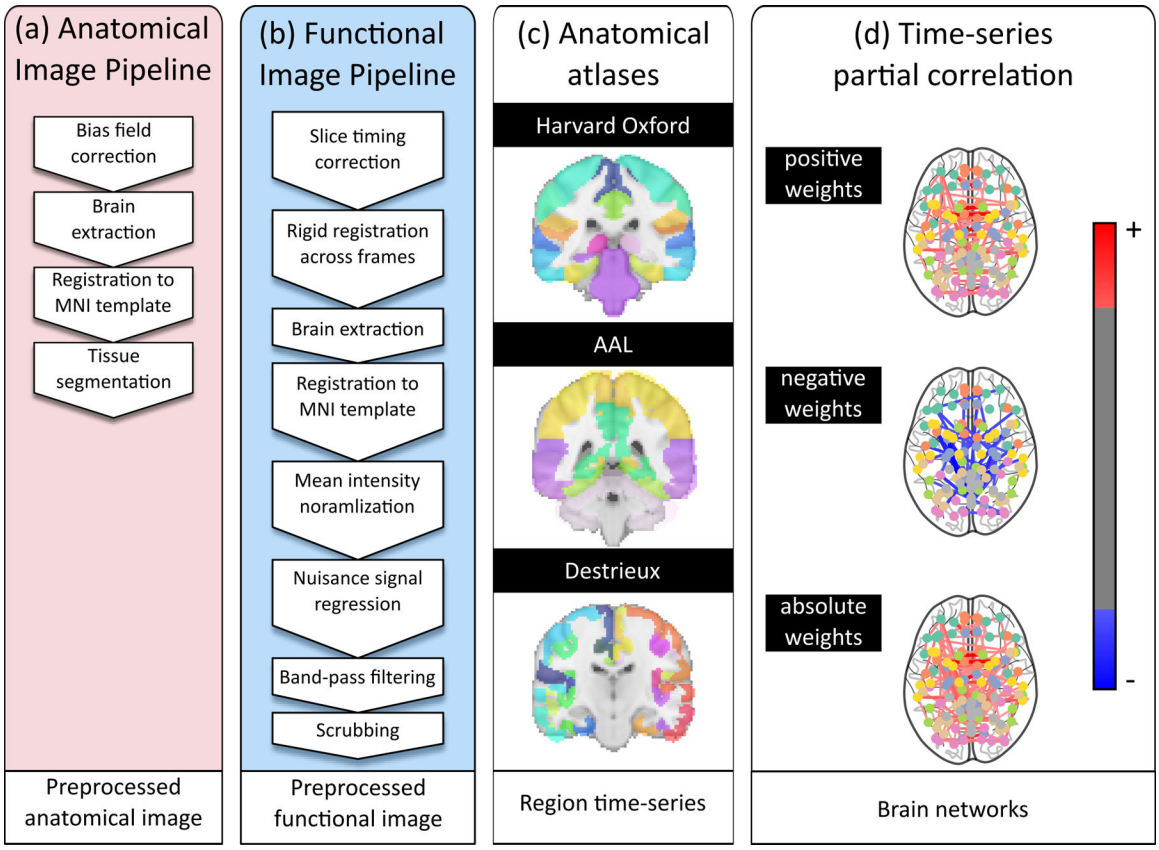

Figure 1:

Overview of the processing pipeline. Each patient's imaging data underwent (a) anatomical processing, (b) functional processing, (c) spatial normalization each of the three atlases, and (d) functional connectome creation.

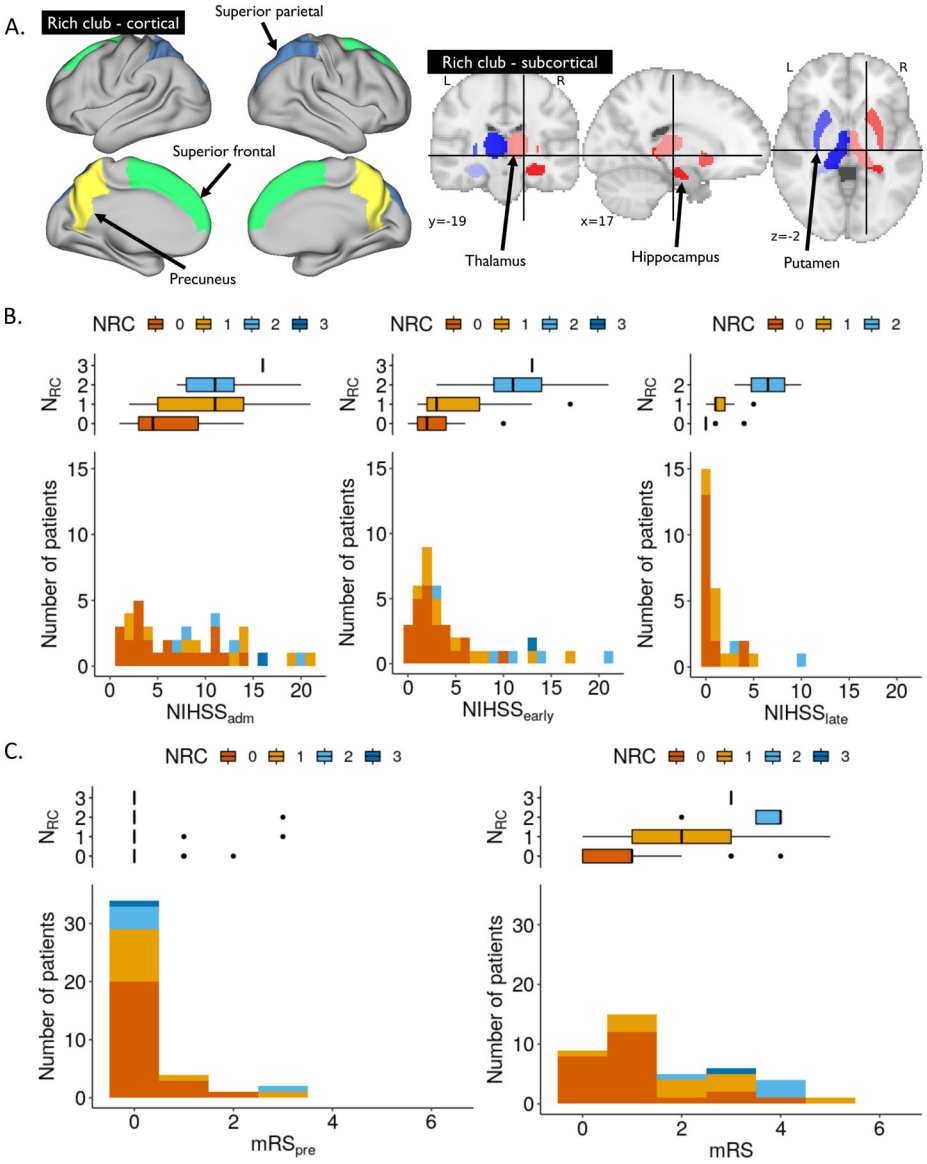

Figure 2:

(A) Visualization of cortical (left) and subcortical (right) RC brain. NIHSS (B) and mRS (C) distributions for all AIS patients, stacked and color-coded by N_{RC}.

Table 1:

Study cohort characterization. Treatment included intravenous tPA or endovascular thrombectomy. There was no difference in patients with and without fMRI data (p>0.2). (sd: standard deviation; IQR: interquartile range)

	SALVO	Patients with fMRI data
n	41	33
N_{RC} (mean (sd))	0.59 (0.81)	0.52 (0.80)
DWIv (cc; mean (sd))	9.13 (12.52)	9.54 (13.49)
Age (years; mean (sd))	69.79 (9.70)	70.03 (10.21)
Sex (male; %)	25 (61.0)	20 (60.6)
mRS_{pre} (mean (sd))	0.29 (0.75)	0.36 (0.82)
mRS (median (IQR); 1 N/A)	1 (2)	1 (2.25)
$NIHSS_{adm}$ (mean (sd); 1 N/A)	8.03 (5.54)	8.28 (5.85)
$NIHSS_{early}$ (mean (sd))	4.85 (4.95)	5.12 (5.34)
$NIHSS_{late}$ (mean (sd); 13 N/A)	1.32 (2.25)	1.29 (2.47)
Stroke location (left; %)	16 (39.0)	11 (33.3)
Treatment (%)	18 (43.9)	13 (39.4)
L^{+}_{HO} (mean (sd))		17.66 (1.01)
L^{-}_{HO} (mean (sd))		20.91 (1.61)
L^{abs}_{HO} (mean (sd))		15.21 (0.92)
L^{+}_{AAL} (mean (sd))		17.57 (1.14)
L^{-}_{AAL} (mean (sd))		20.39 (1.62)
L^{abs}_{AAL} (mean (sd))		14.98 (0.98)
L^{+}_{Des} (mean (sd))		20.12 (1.20)
L^{-}_{Des} (mean (sd))		24.13 (1.95)
L^{abs}_{Des} (mean (sd))		17.62 (1.12)

Table 2:

Summary of outcome models for $NIHSS_{early}$ (top), $NIHSS_{late}$ (middle), and mRS (bottom) with available fMRI data (N=33 and N=21, respectively). Results in parentheses correspond to all available subjects (N=41 and N=28, respectively). For each outcome measure, baseline (top), outcome model (middle), and outcome model without *L* (bottom) are reported. Models that describes the data best are shown in bold.

	Model	R^2	R^2_{adj}	AIC	BIC
$NIHSS_{early}$	$NIHSS_{adm}$	0.64	0.62	190.51	193.44
		(0.62)	(0.61)	(233.98)	(237.36)
	Age+ N_{RC} + L:N_{RC}	**0.81**	**0.79**	**173.55**	**179.42**
	Age + N_{RC}	0.76	0.74	179.84	184.24
$NIHSS_{late}$	DWIv	0.29	0.25	98.78	100.87
		(0.25)	(0.22)	(128.45)	(131.11)
	DWIv + N_{RC} + L:N_{RC}	**0.76**	**0.72**	**80.06**	**84.24**
	DWIv + N_{RC}	0.66	0.62	85.26	88.39
mRS	Age	0.56	0.54	117.44	120.37
		(0.57)	(0.56)	(143.75)	(147.13)
	N_{RC} + L + L:N_{RC}	**0.75**	**0.73**	**102.91**	**108.77**
	N_{RC}	0.56	0.55	144.23	147.61